Characterisation of crowd lateral dynamic forcing from full-scale measurements on the Clifton Suspension Bridge

R.E.White[a], N.A.Alexander[a], J.H.G.Macdonald[a], M.Bocian[b]

[a] Department of Civil Engineering, University of Bristol, Bristol BS8 1TR, UK

[b] Department of Engineering, University of Leicester, Leicester LE1 7RH, UK

Keywords: bridges, dynamics, field testing & monitoring, pedestrian loading, human-structure interaction

November 29, 2019

Abstract

Lateral loading of bridges by a crowd of walking pedestrians is of serious concern as it can lead to a sudden growth in the amplitude of structural oscillations, i.e. lateral dynamic instability. A vibration amplitude threshold, marking a qualitative change in pedestrians behaviour, is then usually proposed beyond which the likelihood of structural instability is said to increase. To verify this presumption, measurements were taken during a crowd loading event on Clifton Suspension Bridge in Bristol, UK. Two lateral modes of the bridge were studied, previously found susceptible to pedestrian-induced excitation. A novel procedure is proposed based on time-frequency analysis enabling, for the first time, the average equivalent added mass per pedestrian to be identified from measurements on a full-scale structure. Previous measurements on Clifton Suspension Bridge during crowd loading leading to the onset of large-amplitude vibrations revealed an increase in the natural frequency of one from the two considered modes. The proposed time-frequency analysis procedure has successfully identified the additional mass, due to the pedestrians, that is effectively negative. Cycle-by-cycle energy analysis per mode confirms the presence of additional damping of the pedestrians at low vibration amplitudes, that is also effectively negative. Although some of the results are uncertain quantitatively, there is no evidence of the amplitude threshold at which the human-structure interaction phenomenon occurs.

1 Introduction

Human-Structure Interaction (HSI) is a phenomenon of increasing interest for researchers from civil, structural and mechanical engineering disciplines. The literature has documented many cases of large amplitude lateral bridge oscillations in the presence of pedestrians. The most comprehensive studies include the London Millennium Footbridge (LMF) [1], Toda Park Bridge (TPB) [2], Solferino Footbridge (SF) [3], Pedro e Inês Footbridge [4], Clifton Suspension Bridge (CSB) [5] and the Singapore Airport Changi Mezzanine Bridge (CMB) [6]. The cause of excessive response of these bridges is thought to be negative damping provided by pedestrians. The framework of modelling humans as negative dampers was first suggested by Arup [1] from analysis of the experimental data on the behaviour of LMF. This framework was expanded to account for the component of pedestrian force in phase with structural acceleration (or displacement) after some tests on an instrumented treadmill by Pizzimenti and Ricciardelli [7]. After scaling, this force component can be expressed as equivalent added mass (or stiffness). While added damping and stiffness are conventionally adopted in wind engineering when modelling aeroelasticity, [8] [9], it is not entirely clear how these force components arise from the action of a crowd. Nevertheless, in the human structure interaction literature [1, 5, 6, 7, 10, 11, 12, 13, 14, 15] it is conventional to model the effects of pedestrians as equivalent added damping and mass or stiffness (which can be positive or negative) to the structure. A plausible explanation of the added damping effect was provided by Macdonald [10] who, expanding a simpler model by Barker [16], built a highly reduced order pedestrian model inverted pendulum model (IPM). The IPM can capture pedestrian dynamics in the frontal plane when walking on a rigid ground [17, 18]. When applied to a laterally oscillating structure, IPM is capable of generating negative added damping and hence cause the onset of divergent amplitude vibrations, even without pedestrians synchronising their stride frequency to that of the structure [10, 19].

1.1 Negative damping model

Controlled pedestrian loading tests were carried out on the LMF in which the density and number of walkers were varied [1]. Detailed analysis of the collected data revealed that the lateral force amplitude per pedestrian is approximately linearly correlated to the local lateral velocity amplitude of the deck. The linear force-velocity relationship implied that lateral pedestrian loading could be treated as equivalent to the action of negative dampers that tend to amplify the bridge responses. Thus, Arup proposed that it was a result of pedestrians acting as ‘negative dampers and synchronising with bridge motion’ which caused

the growth of large amplitude dynamic vibrations, termed a lateral instability [1]. Using data from the full-scale tests, Arup were able to estimate the average negative damping coefficient per pedestrian. They named this the'lateral walking force coefficient', k (see [1]). If each person introduces negative damping, then when N_{crit} pedestrians are on a structure the sum of pedestrians and structural damping equals zero, for a given mode. Thus, the formulation (eqn. (1)) estimates the number N_{crit} of pedestrians, having uniform spatial density, that is necessary to generate a structural system with zero total modal damping. Any pedestrian number greater than this N_{crit} would result in a growth of large amplitude dynamic vibrations.

$$N_{q,crit} = \frac{4\pi f_{q,n}\zeta_{q,b}M_{q,b}}{k\psi}, \qquad \psi = \int_0^{L_b} \frac{1}{L_b}\phi_q^2(x)\mathrm{d}x \tag{1}$$

where $f_{\text{q,n}}$ is the modal natural frequency [Hz], $\zeta_{\text{q,b}}$ is the damping ratio, $M_{\text{q,b}}$ is the bridge modal mass, k is the negative damping coefficient per person, ψ accounts for the distribution of pedestrians along the bridge, L_{b} is the length of the bridge, $\phi_q(x)$ is the lateral mode shape and x is the coordinate along the bridge length, and q is the mode number. For uniform mass per unit length, the bridge modal masses, $M_{\text{q,b}}$, are defined as

$$M_{q,b} = \frac{M_b}{L_b}\int_0^{L_b} \phi_q^2(x)\mathrm{d}x \tag{2}$$

where M_{b} is the overall bridge mass.

Using the value of k = *300*Ns/m derived from the LMF [1] it was possible to predict the number of people for which the initiation of large amplitude vibrations occurred in the case of the Pedro an Inês Footbridge in Portugal [4]. Measurements taken on the Changi Mezzanine Bridge [6] and Clifton Suspension Bridge [5] agreed with the above negative damping model, although the derived values of the damping coefficient differed. The initiation of divergent lateral vibrations on the Clifton Suspension Bridge was found to occur for 150 and 240 pedestrians for the second and third lateral mode, respectively. It was estimated that 70 pedestrians were required for the onset of large amplitude vibrations to occur on the Changi Mezzanine Bridge [6].

1.2 Aims

This paper explores the amplitude dependency for the observed effects of HSI from measurement taken on the Clifton Suspension Bridge. The frequency spectrum is investigated during the crowd loading event to identify any subtle HSI effects, including shifts in natural frequencies. The aim is to determine negative or positive equivalent added damping and mass due to pedestrians contributing to the lateral bridge response. A novel application of the Hilbert transform is employed to estimate the added mass and damping due to HSI. New results presented here, from a crowd loading event in 2017, are compared with previous data collected during the International Balloon Fiesta in 2003 [5].

The aims of this paper are to explore the following research questions:

- Is human-structure interaction observed at low-amplitude lateral bridge vibration?
- Is Arup's negative damping model applicable for low-amplitude lateral bridge vibrations?
- Counter intuitively, can a structure's modal mass appear to decrease with an increase of pedestrian numbers?

2 Experimental method

An experiment on the Clifton Suspension Bridge, Bristol, England, was carried out on Sunday 15th October 2017. A structural health monitoring system (SHM) was deployed to investigate the bridge response during the crowd loading event. Crowd monitoring by GoPro video cameras was carried out in synchrony with the SHM.This experiment was reviewed by the faculty research ethics board. The size and structure of the bridge also makes it convenient for study: small enough that the complete bridge can be monitored and understood, but large enough and flexible enough to exhibit some interesting dynamic behaviour [5, 9].

2.1 Bridge description

The Clifton Suspension Bridge spans the River Avon bridging from Clifton, Bristol, to Leigh Woods, North Somerset. It is approximately 2km west of the centre of Bristol. The main span is 214.35m,

from centreline to centreline of the towers, with the suspended bridge length spanning 193.85m, L_b. The roadway is 6.1m wide between the two longitudinal stiffening girders. These are supported by vertical suspension rods spaced 2.44m apart from each other along the bridge. Total deck width is 9.46m including 1.1m footways either side. The deck design comprises of timber with wrought iron lattice cross-girders. Lateral restraint is provided at either end by a tongue and groove design. No direct vertical or torsional restraint is provided by the abutment; the vertical loads are fully carried by the suspension rods allowing for relative motion. The chains account for approximately half the dead load of the main span. The overall bridge mass is approximately 1150 tonnes, M_b. A more complete description of the structure is given by Barlow [20]. The bridge layout and locations of the monitoring instruments are displayed in Figure 1.

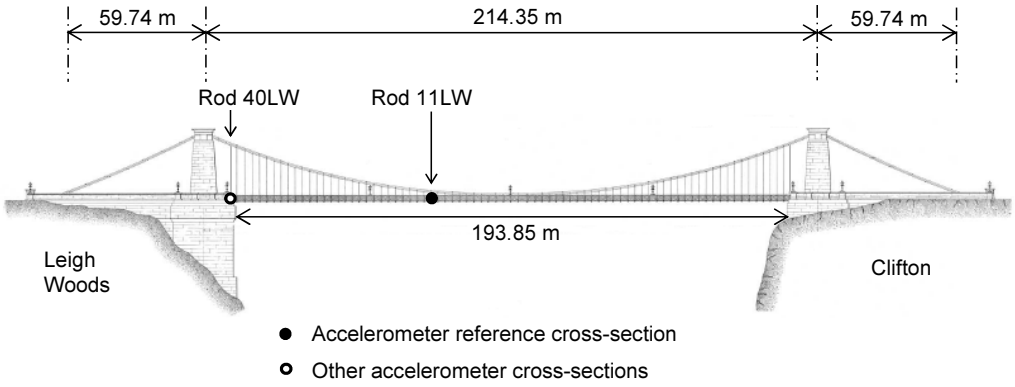

Figure 1: *Clifton Suspension Bridge diagram with associated rod(hanger) references, based on a figure from Barlow [20] (used with permission)*

2.2 Structural health monitoring (SHM) system and data acquisition

The SHM was setup at two (hanger) locations, illustrated in Figure 1, Rod 11LW and Rod 40LW. Rod 11LW, located 26.7m from the bridge midpoint, was previously identified by Macdonald [5] as a suitable point for motion measurement in all lateral vibration modes below 3Hz. Rod40LW was selected as it was believed that this would show the greatest vertical transient response from pedestrians exciting the suspended deck span [21]. The CSB is well documented and previous work carried out by both Macdonald [5] and Gunner et al. [21] allowed for the efficient installation in one afternoon only requiring four people.

The sensors used as part of the SHM comprised of four accelerometers, including three uniaxial (Tokyo

measuring instruments lab) ARF-A low capacity acceleration transducers and a single triaxial accelerometer, (Lord Microstrain) G-LINK-200-8g, and two displacement transducers. At Rod 40LW the triaxial accelerometer was positioned above bridge deck level. Parallel to this, two displacement transducers and a single acceleration transducer were positioned below bridge deck level on the articulation span. These measured vertical displacements and accelerations. At Rod 11LW, three uniaxial accelerometers were positioned below bridge level. Two of these measured vertical motions on either side of the bridge deck, from which the pure vertical and torsional components of motion could be determined. The third accelerometer measured lateral accelerations. Sampling was configured to a rate of 64 Hz.

Four GoPro cameras were set up, two at either end of the bridge, mounted on the towers above pedestrian level. The GoPro data analysis was carried out to correlate the manual pedestrian counts and to ensure the validity of the timestamp data. An FE (Finite Element) model has been previously constructed by COWI [22] for the Clifton Suspension Bridge corresponding to the unloaded case. This model has been employed to estimate the mode shapes and modal masses for the lateral modes of interest. Modes shapes were scaled to a maximum amplitude of unity. Table 1 characterises the second and third lateral modes with the corresponding mode shapes shown in Figure 2. Lateral modes are labelled L1, L2, L3 etc, where L1 is the lowest frequency lateral mode. Modes L2 and L3 were found to have the lowest damping ratios which is significant as these modes experienced large-amplitude pedestrian-induced vibrations during the Balloon Fiesta in 2003 [5]. It is not surprising that these two modes were thus excited again during this crowd loading event.

Table 1: *Lateral bridge modes L2 and L3, using COWI's Finite Element model [22]*

Mode	Modal frequency, $f_{\mathrm{q,n}}$ [Hz] (measured [5])	Modal damping ratio, $\zeta_{\mathrm{q,b}}$ [%] (measured [5])	Modal mass, $M_{\mathrm{q,b}}$ [tonnes] (FE [22])
L2	0.524	0.580	691.9
L3	0.746	0.680	698.7

2.3 Crowd monitoring

The crowd loading event took place for a duration of 19 minutes between 11:29am and 11:48am. The bridge was closed to all vehicles during the event, allowing pedestrians to walk along the roadway. Low volume footpath traffic was active with pedestrians not taking part in the prescribed event. GoPro footage showed that pedestrian flow along these pathways exhibited larger walking speeds than pedestrians travelling along the roadway. Pedestrians were limited to groups of 25, set off at 30s intervals, with

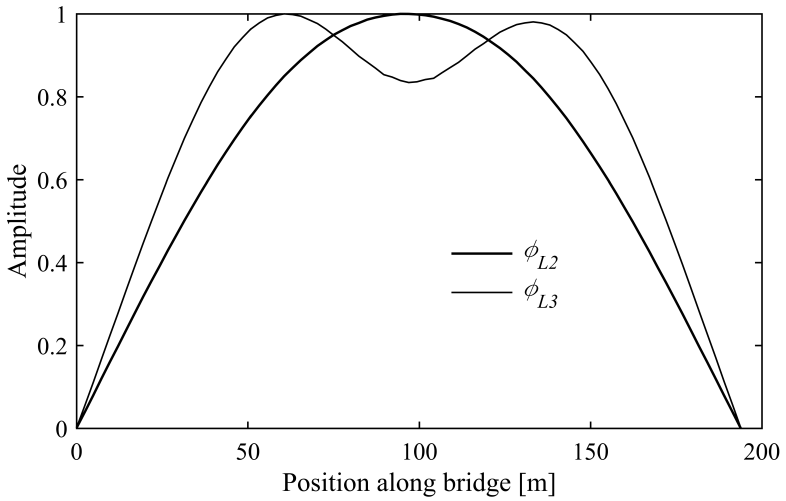

Figure 2: *Clifton Suspension Bridge lateral mode shapes L2 and L3 identified using COWI's Finite Element model [22, 5]*

the aim of limiting the total number of pedestrians on the bridge, given the large amplitude vibrations experienced during the previous crowd loading event [5]

To measure the number of pedestrians on the bridge as a function of time, four team members counted the flow of people using the smartphone timestamp application TimeStamp [23]. Two team members were situated at each end of the bridge, counting people stepping onto or off the suspended span, since the pedestrian traffic was bi-directional. The positive direction of progression was defined as Clifton to Leigh Woods. Pedestrians moving in the opposite direction (Leigh Woods to Clifton) were denoted as a counter-flow. This was found to be as low as 1-4 pedestrians on the bridge at any one time and could therefore be assumed to be negligible in the analysis. A total of 780 people were recorded crossing the bridge over the 19-minute period. This included pedestrians not participating in the official event. The number of people on the bridge as a function of time was evaluated using the summation of the people counted on (Clifton) and off (Leigh Woods). At any time during the event the maximum total number of people on the bridge was 151. This includes people on both the roadway and footways. This number was only sustained for short time periods with the number fluctuating greatly, as can be seen in Figure 3.

2.4 Crowd dynamics and kinematics

The average velocity of each pedestrian was estimated using the raw timestamp data [23] assuming there was, on average, no overtaking on the bridge. The corresponding positions of each individual pedestrian

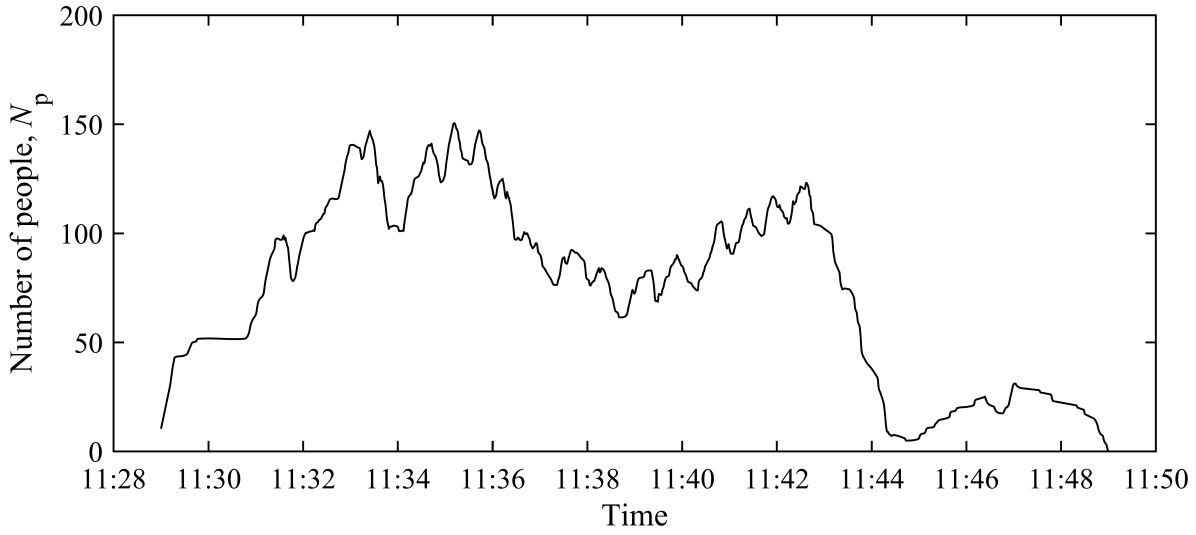

Figure 3: *Number of people on the Clifton Suspension Bridge during the crowd loading event*

along the suspended bridge length, as a function of time, during the crowd loading event were evaluated as,

$$x_j(t) = (t - t_{\text{arr,j}})v_j, \qquad v_j = \frac{L_b}{t_{\text{dep,j}} - t_{\text{arr,j}}} \tag{3}$$

where $x_j(t)$ is the position of the j^{th} pedestrian, t is time, $t_{\text{arr},j}$ and $t_{\text{dep},j}$ are the arrival and departure times of the j^{th} pedestrian respectively. v_j is the estimated average velocity of the j^{th} pedestrian.

During the crowd loading event pedestrians were found to take, on average, 102.5s to cross the 193.85m suspended span. This equates to an average walking speed of 1.89m/s, which is larger than the typical preferred walking speed for humans, which is roughly 1.4m/s [24, 25]. However, humans are capable of walking at speeds upwards of 2.5m/s, and there were a few runners during the event which would increase the average speed [26]. Individuals find slower or faster speeds uncomfortable. This too agrees with data collected and analysed by Pachi and Ji [27]. Their results indicated pedestrian's walked over footbridges in the velocity range 0.93-1.8m/s.

2.5 Effective number of people (per mode) distributed on bridge

The effective number of people loading each mode accounts for the distribution of pedestrians on the bridge relative to the mode shape. Using mode shapes L2 and L3, shown in Figure 2 it was possible to estimate the effective number of people, $N_{q,\text{eff}}$, contributing to each mode of interest as follows

$$N_{q,\text{eff}} = \sum_{j=1}^{N_p} \phi_q^2(x_j(t)) \tag{4}$$

where $N_{q,\text{eff}}$ is the effective number of people loading the q^{th} mode and N_p is the number of people. For uniformly distributed pedestrians the effective number is found to be roughly half the total number, on the bridge at that time, based on the mode shapes normalised to a maximum magnitude of one. The maximum effective number of people during the crowd loading event at a given time was found to be 87 and 94 people for modes L2 and L3 respectively. These correspond to 58% and 39% of the pedestrians required for the onset of large amplitude vibrations ($N_{crit} > N_p$) according to equation (1), based on $k = 300Ns/m$). This is represented in Figure 4 showing the effective number of people for both modes as a function of time during the crowd loading event.

The mass ratio, μ_q, (for the q^{th} mode) is the ratio of the pedestrian modal mass to the structural modal mass for a particular mode and is defined as,

$$\mu_q = \frac{M_{q,p}}{M_{q,b}} \tag{5}$$

where the pedestrian modal mass is $M_{q,p}$ is defined as,

$$M_{q,p} = \sum_{j=1}^{N_p} m_j \phi_q^2(x_j) \approx \bar{m}_p \sum_{j=1}^{N_p} \phi_q^2(x_j) = \bar{m}_p N_{q,\text{eff}} \tag{6}$$

where m_j is the mass of the j^{th} pedestrian and $\bar{m}_p$ is the average pedestrian mass. It should be noted that each pedestrian is modeled as a lumped mass m_j, in equation 6, where m_j is the actual total mass of the j^{th} pedestrian. We make no attempt to model each pedestrian in a more complex biomechanical fashion as a multi-degree of freedom system.

National Health Service (UK) statistics report that the average mass of the general population, in the UK, is approximately 76kg [28]. Assuming this value for the average pedestrian mass, $\bar{m}_p$, the pedestrian modal mass, $M_{q,p}$, can be simply evaluated by multiplying it by the effective number of people, seen in Figure 4, as indicated in eqn. (5). The maximum modal pedestrian masses are then estimated to be 6.38 tonnes for mode L2, and 6.31 tonnes for mode L3, occurring at approximately 11:33am and 11:35am respectively. These correspond to mass ratios of 0.0096 and 0.0102 respectively.

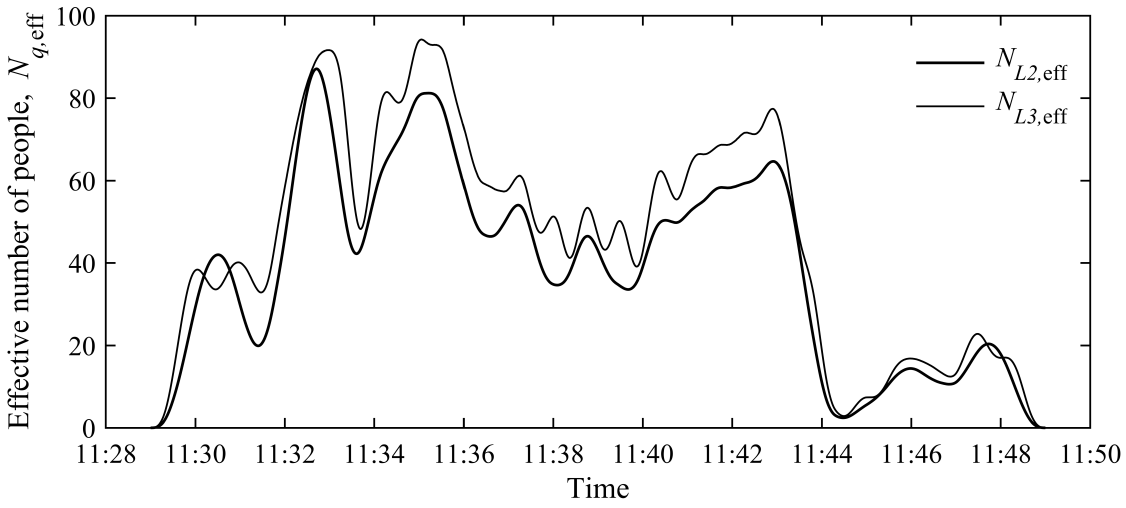

Figure 4: *Effective number of people loading modes L2 & L3 during the event*

3 Experimental data analysis

A 40-minute window of data collected by the structural health monitoring system was retrieved around the crowd loading event. Figure 5 shows the complete band-pass filtered lateral acceleration time-history, measured at Rod 11LW, illustrating five periods of differing loading. The band pass filter contained a low-cut filter at 0.2Hz (to remove quasi-static effects, [5]) and a high-cut filter at 5Hz (as only low-frequency modes are of interest).

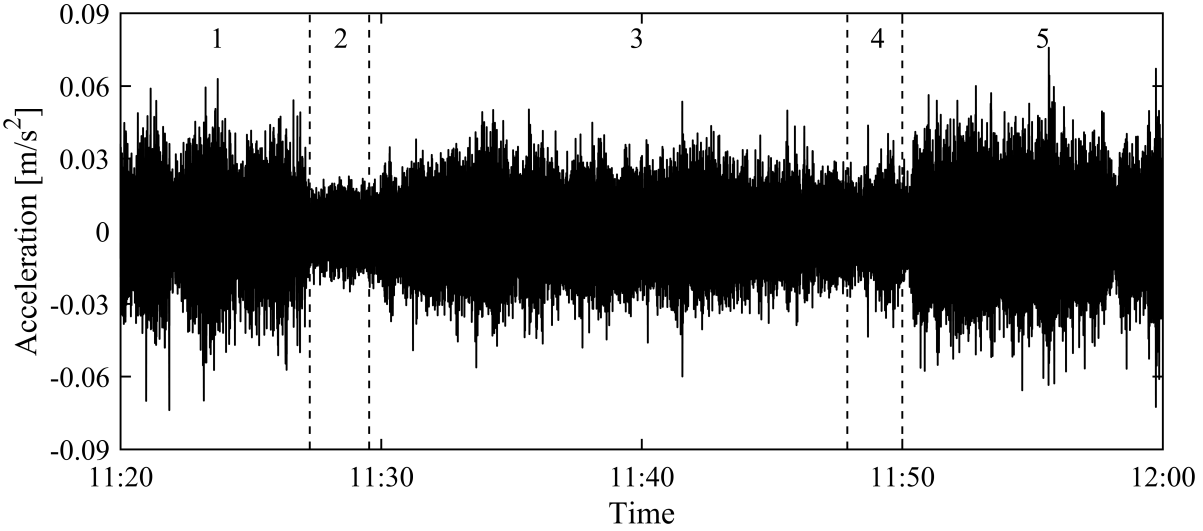

Figure 5: *Band-pass filtered lateral acceleration at Rod 11 of the Clifton Suspension Bridge over 40min period of monitoring*

Table 2 identifies the loading conditions for each of the five periods. This allowed for efficient post-processing of the data in comparing the conditions of the bridge before, during and after the crowd

loading event. Using these specified conditions, the data were split into three datasets corresponding to periods 1, 3 and 5 respectively. Note that the ambient ('unloaded') vibration cases 2 and 4 were not long enough in duration to extract useful resolution frequency information for the modes of interest, so are not considered here. Differences in the power spectral densities could then be identified between the vehicle and pedestrian loading conditions. The implications of these are discussed in Section 3.1. The maximum lateral acceleration observed during the crowd loading event was approximately 2.35 times the maximum response in ambient conditions.

Table 2: *Sections of measurements corresponding to band-pass filtered lateral acceleration time-history in Figure 5*

Period	Description	RMS Acceleration (m/s^2)	Key Times
1	Traffic loading	0.013	Bridge Closure: 11:27
2	Unloaded (nominal conditions)	0.007	Start of crowd event: 11:29
3	Crowd loading event	0.011	End of crowd event: 11:48
4	Intermediate loading	0.009	
5	Traffic loading	0.014	Bridge Reopened: 11:50

3.1 Data Processing

To investigate the crowd loading effects on specific critical modes, the response accelerations were band-pass filtered in the frequency ranges 0.45-0.65 Hz and 0.65-0.83 Hz to isolate the responses of modes L2 and L3 respectively. The filters used were zero-phase 6th order Butterworth filters. The amplitude envelopes of these band-filtered responses are displayed in Figure 6 for the crowd loading period (period 3 in Figure 5 and Table 2). The amplitude envelope in this figure was obtained using the Hilbert Transform [29, 30]. The short-time Fourier transform [31] is not used because it suffers from a loss of time-frequency resolution due to the Heisenberg's uncertainty principle. The Hilbert transform allows a much higher time-single frequency resolution. Section 3.2 discusses the implementation of the Hilbert transform used in this paper.

Table 3 summarises the maximum lateral dynamic responses measured at Rod 11LW for both crowd loading events. Displacements estimates were calculated by double integration of the measured acceleration at Rod11LW. There is a significant difference in magnitude of the amplitudes observed during each crowd loading event. The 2003 event had an estimated maximum number of 488 pedestrians on the bridge, at any one time, equating to an average pedestrian density over the two footways of 1.1people/m^2, the roadway was kept closed. In contrast, the 2017 event had a maximum number of 151 pedestrians

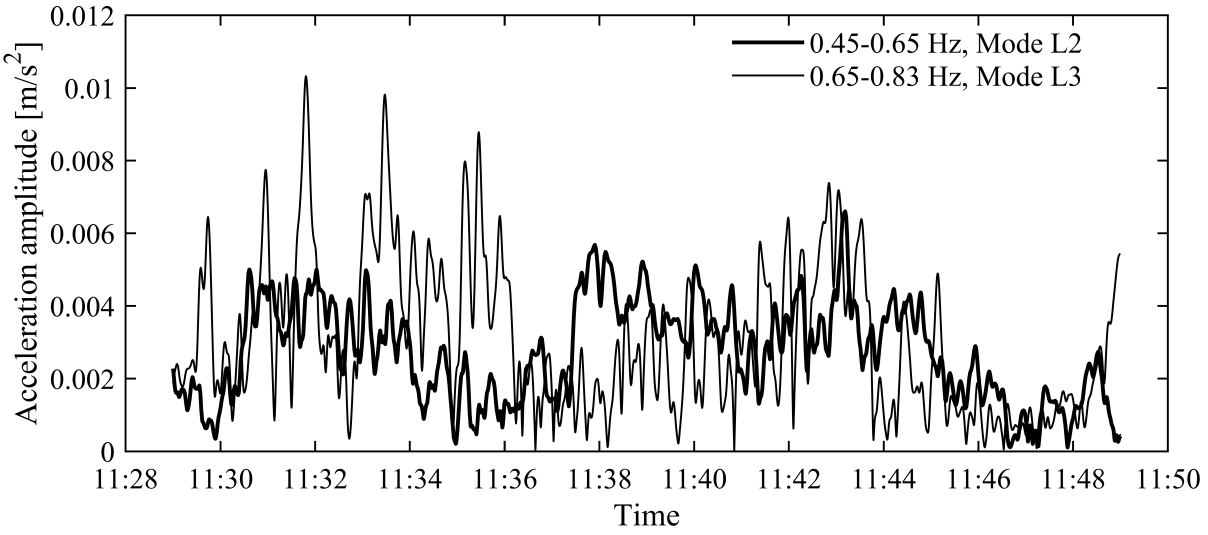

Figure 6: *Acceleration amplitude envelopes for lateral modes L2 and L3 during crowd loading period*

on the bridge, at any one time. The average pedestrian density over the roadway was found to be 0.13 people/m^2. An advantage of the 2017 data is that pedestrians were counted on and off the suspended bridge span, so the pedestrian numbers are reliable, whereas for the 2003 data the pedestrian numbers were only estimated from CCTV footage of people approaching the bridge.

Table 3: Comparison of maximum lateral dynamic responses measured at Rod 11LW

	2003 event [5]		2017 event	
	Peak Disp.	Peak Acc.	Peak Disp.	Peak Acc.
	mm	m/s^2	mm	m/s^2
Total (0.2-5Hz)	11.7	0.190	1.5	0.054
Mode L2 (0.45-0.65 Hz)	10.2	0.110	0.59	0.007
Mode L3 (0.65-0.83 Hz)	4.7	0.110	0.43	0.010

‘

Figure 7 displays the power spectral density (PSDs) of lateral accelerations (using Welch’s algorithm [32]) for the time periods before (period 1), during (period 3) and after (period 5) the event. These power spectra indicate small increases in frequency of mode L2 and L3 modes during the event. This may be due to fact that the traffic loading (in periods 1 and 5) has a larger mass than the crowd (in period 3). The resonance peaks of L2 and L3 modes appear to be slightly narrower for crowd loading than for traffic loading. This is suggestive of a reduction in damping, although the frequency resolution of the spectra is not sufficient for robust estimates of damping to be made from them. The spectral power observed around 0.3-0.4Hz is the lateral component of torsional mode ‘T1’ (0.356Hz), as identified by Macdonald [5].

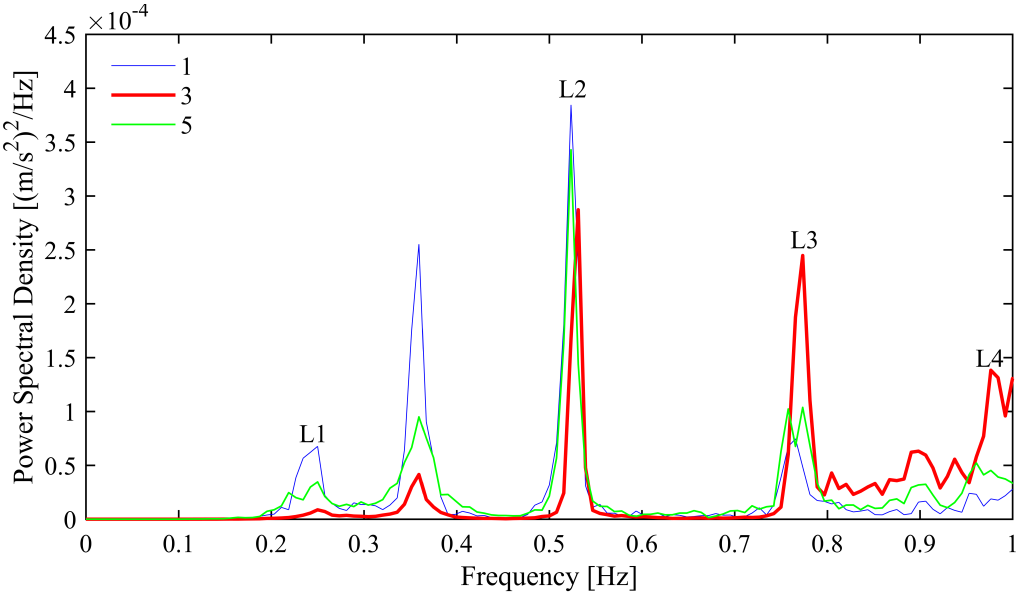

Figure 7: *Power Spectral Densities of lateral acceleration with labelled modes of vibration*

3.2 Time-Frequency Analysis: Hilbert Transform

By using the Hilbert transform the time-varying (instantaneous) phase, frequency, and amplitude (envelope) of a real time-series can be calculated. The analysis of the instantaneous frequency allows the characterisation of any fluctuations observed in the bridge modal frequencies. These fluctuations could illustrate the presence of equivalent added mass (negative or positive) of the pedestrians, even at low-amplitudes. The modal acceleration signals of L2 and L3, during period 3 of Figure 5 and Table 3 (11:29 - 11.49), were used for the time-frequency analysis, Hilbert transform. These transformed signals were used to characterise the mean equivalent added mass per pedestrian.

Formally, let $x(t)$ represent a timeseries. An analytical signal $s(t)$ of this timeseries $x(t)$ (computed directly using the *hilbert()* function in Matlab [29, 30]), is defined as

$$s(t) = x(t) + \mathrm{iy(t)} \tag{7}$$

where $y(t)$ is the Hilbert transform of $x(t)$ and $\mathrm{i} = \sqrt{-1}$. The instantaneous natural frequency is given by,

$$f(t) = \frac{1}{2\pi}\frac{\mathrm{d}\theta(\mathrm{t})}{\mathrm{dt}}, \quad \theta(t) = \arctan\left(\frac{y(t)}{x(t)}\right) \tag{8}$$

where $f(t)$ and $\theta(t)$ are the instantaneous natural frequency and phase respectively. The instantaneous

amplitude envelope is given by

$$A(t) = |s(t)| = \sqrt{x(t)^2 + y(t)^2} \tag{9}$$

Eqn. (8) can be further expanded (using complex number algebra, see [33]) as

$$f(t) = \frac{1}{2\pi} \frac{x(t)\dot{y}(t) - y(t)\dot{x}(t)}{A(t)^2} \tag{10}$$

This form avoids the direct use of the *arctan()* function. It also indicates three key problems with this instantaneous frequency estimate, that are

(i) The instantaneous frequency estimate is a single-valued function in time. Hence, it is only possible to estimate one instantaneous frequency at a particular point in time t. In the case of multi-frequency component signals $x(t)$ eqns (8) and (10) will produce some weighted average of all components at t.

(ii) Computing $y(t)$ from $x(t)$ makes use of the Fast Fourier Transform (FFT) and this is subject to its well documented spectral leakage [34]. For finite length signals spectral leakage can introduce significant errors in the instantaneous frequency at the beginning and end of the signal.

(iii) When the amplitude of the signal $A(t)$ tends to zero it is likely that the frequency estimate will tend to $\pm\infty$. This leads to spikes in instantaneous frequency estimates.

To alleviate these three problems the follow strategies have been adopted:

(i) The instantaneous frequencies for a single modal acceleration component $\ddot{x}_q$ are calculated, that is obtained by band-pass filtering previously discussed. Therefore, we limit the averaging of multi-components signals

(ii) The filtered (mode q) acceleration signal $\ddot{x}_q(t)$ is multiplied by a Tukey windowing function $w\,(t)$ to attenuate (spectral leakage) at the beginning and end of the signal

(iii) A threshold is applied to the instantaneous frequency data f_q. This means the validity of the instantaneous frequency estimate is only accepted if its corresponding instantaneous amplitude is above a threshold level. A threshold value of 25% of signal maximum was found to be a reasonable

compromise between spike removal while keeping a large enough sample size. Equation (11) defines thresholding

$$f_q(t) = \begin{cases} f_q(t) & : \quad A_q(t) > 0.25\max(A_q(t)) \\ \emptyset & : \quad otherwise \end{cases} \tag{11}$$

where $\emptyset$ signifies a null set, i.e. not a number (NaN) within MatLab.

The thresholded amplitudes and instantaneous natural frequencies of mode L2 and L3 are illustrated in Figure 8 and 9 as green lines overlaying the instantaneous amplitude and natural frequency (black lines in both Figure 8a, 8b, 9a and 9b). The thresholded quantities are taken as 25% of each maximum modal acceleration response corresponding to 0.007m/s^2 and 0.010m/s^2, for modes L2 and L3 respectively.

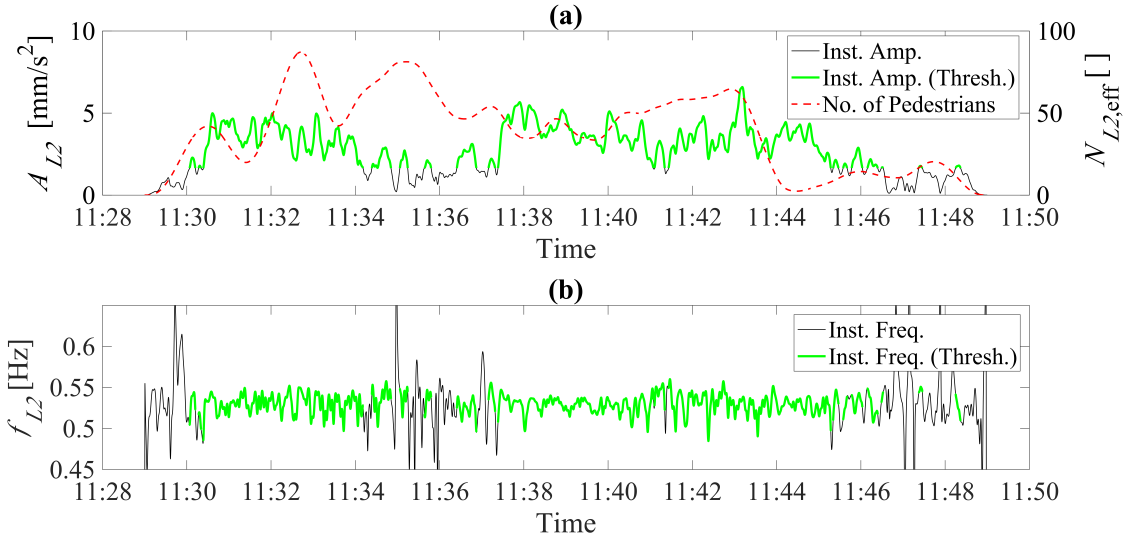

Figure 8: *Comparison plots, Mode L2 (a) Instantaneous Amplitude, effective number of Pedestrians vs time (b) Instantaneous natural frequency vs time*

3.3 Statistical analysis of Human-Structure Interactions

The bridge modal responses for the 2017 crowd loading event are low in amplitude and the number of pedestrians are well below the critical threshold ($N_p < N_{\text{crit}}$). Nevertheless, statistical analysis is performed to determine whether there is any evidence suggestive of a correlation between the effective number of people, the observed instantaneous amplitudes and natural frequencies, for modes L2 and L3.

Figures 8 and 9 show a direct comparison between the pedestrian loading numbers ($N_{q,\text{eff}}$) and estimated

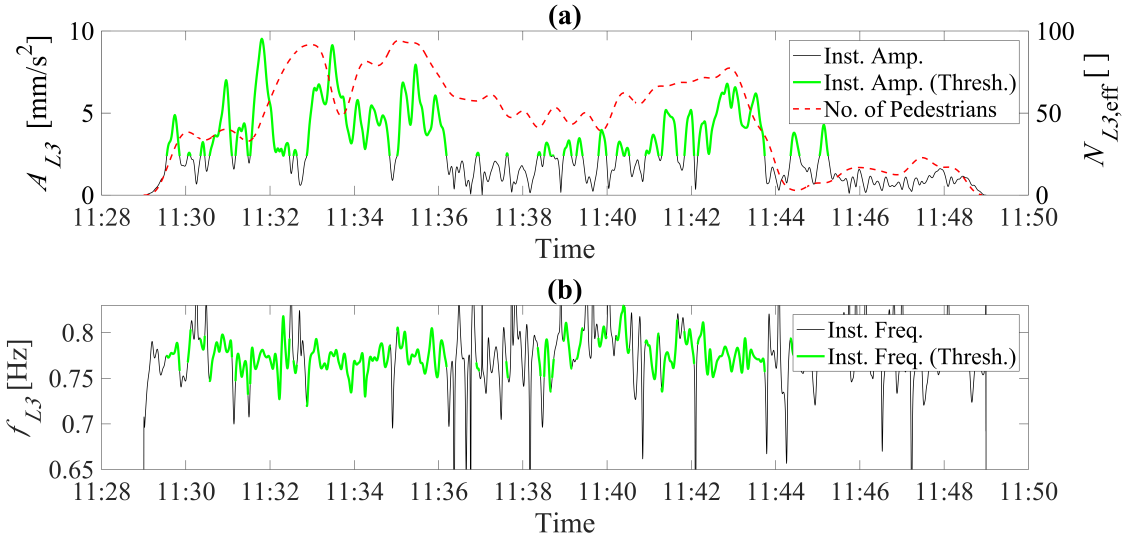

Figure 9: *Comparison plots, Mode L3 (a) Instantaneous Amplitude, effective number of Pedestrians vs time (b) Instantaneous natural frequency vs time*

bridge's instantaneous amplitude A_q and natural frequency f_q of mode q). The correlations between these quantities are determined by evaluating the Pearson correlation coefficient r [35]. Table 4 displays the respective correlation coefficients of the instantaneous amplitude and natural frequency with the effective number of people, for lateral modes L2 and L3. The fourth column identifies the minimum value required for the correlation, between the effective number of people and instantaneous frequency, to be considered statistically significant [36].

A correlation exists between the instantaneous response amplitude A_q and effective number of pedestrians $N_{q,\text{eff}}$ for mode L3. There is a weaker correlation between instantaneous natural frequency and effective number of pedestrians, although still significant (statistically at a 99% confidence level, as shown in Table 4). However, in Figure 8, the increase in the effective number of people is subtly mirrored in the instantaneous natural frequency and amplitude in the time 11:30-11:34am for mode L2. The interesting finding here is that the correlation between $N_{q,\text{eff}}$ and f_q for mode L2 is positive while it is negative for mode L3.

Table 4: Correlation coefficients for comparisons of instantaneous frequencies and amplitudes with the effective number of pedestrians

	Pearson correlation coefficients		
	Inst Freq. $f_q(t)$	Inst. Amp. $A_q(t)$	Significant r at 99% confidence
$N_{L2,\text{eff}}$	0.123	0.252	0.019
$N_{L3,\text{eff}}$	0.130	0.549	0.014

3.4 Estimating effective added mass per mode $M^*_{q,p}$

In this section we first estimate the change in modal frequencies due to the addition of the pedestrian masses from a theoretical point of view. We then seek to validate this expression (modal frequency change vs. the effective number of pedestrians) with experimental data. Results indicate that pedestrians appear to acts as both positive or negative equivalent added mass.

The equivalent added mass is estimated through fluctuations in the bridge modes' instantaneous natural frequencies. The unloaded natural modal frequency of mode q is given as

$$f_q = \frac{1}{2\pi}\sqrt{\frac{K_{q,b}}{M_{q,b}}} \tag{12}$$

where $K_{q,b}$ is the bridge modal stiffness.

Treating the crowd simply as added mass, the loaded natural modal frequency of mode q is given by

$$2\pi f_q^* = \sqrt{\frac{K_{q,b}}{M_{q,b}+M_{q,p}^*}} = \sqrt{\frac{K_{q,b}}{M_{q,b}\left(1+\alpha_q\mu_q\right)}} = \sqrt{\frac{K_{q,b}}{M_{q,b}}}\left(1+\alpha_q\mu_q\right)^{-\frac{1}{2}} \tag{13}$$

Using the binomial expansion, for the case of small μ_q, we obtain the follow estimated change in the natural frequency due to the crowd

$$f_q^* \simeq f_q\left(1-\tfrac{1}{2}\alpha_q\mu_q+\mathcal{O}\left({\mu_q}^2\right)\right) \tag{14}$$

where $M^*_{q,p}$ is the effective crowd modal mass which is equal to $\alpha_q M_{q,p}$, that is a certain proportion α_q of the crowd modal mass $M_{q,p}$ given in eqn (6). The modal mass ratio of crowd to bridge is μ_q and is defined in eqn (5). This mass ratio can also be expressed in terms of the effective number of people $N_{\text{eff,q}}$, average person mass $\bar{m}_p$ and the bridge modal mass $M_{q,b}$ hence

$$f_q^* \simeq f_q - \alpha_q\left(\frac{f_q\bar{m}_p}{2M_{q,b}}\right)N_{q,\text{eff}} = a + bN_{q,\text{eff}} \tag{15}$$

Equation (15) demonstrates a linear relationship between the effective number of pedestrians (for mode q), $N_{q,eff}$, and the instantaneous modal natural frequency f_q^*. The coefficients of the linear fit, hla and

b, are the intercept and gradient respectively.

Figures 10 and 11 illustrate the relationships between the effective number people and instantaneous frequency for modes L2 and L3 for both low and high amplitude response crowd loading events, in 2017 and 2003 respectively. Figures 10(a) and 11(a) both show a positive linear correlation however the gradient values for mode L2, indicated in Table 5, are dissimilar. The 95% confidence limits of Figure 10(a) are significantly larger than Figure 11(a) suggesting tentative evidence for equivalent added mass by pedestrians during the 2017 crowd loading event. The linear trend in Figure 11(a) is very clear. The scatter of data in these figures can be partly explained by the instantaneous fluctuations in pedestrian stepping behaviour which can cause the equivalent added mass to vary from step to step. Nevertheless, when averaged over a long time record, this would reveal the underlying relationship between the instantaneous natural frequency, hence equivalent added mass, and the effective number of people.

Evaluating the mean equivalent added mass per person, $\alpha_q \bar{m}_p$, using equation 15, we obtain values of -164kg and for -71.5kg. These are considerably different. During the 2003 crowd loading event a significant number of people were observed over a greater time span which would suggest a larger pedestrian density. This correlates to slower pedestrian walking speeds, which according to the IPM, changes the equivalent added mass (and damping) per person [19]. In comparison, the recent crowd loading event observed less people interacting on the bridge over a shorter time span equating to a much smaller pedestrian density promoting larger pedestrian walking speeds. According to the IPM, mode L2's natural frequency, 0.524Hz, is within the bandwidth where the equivalent negative added mass is negative [19].

The correlations of mode L3 in Figures 10(b) and 11(b) are inconclusive however there is some tentative suggestion for the presence of equivalent added mass by pedestrians. A negative linear correlation is observed for the 2017 event whilst a positive linear trend is illustrated for the 2003 event. Evaluating the mean equivalent added mass per person, using eqn 15, we obtain values of -6.7kg and 174kg. The gradient of mode L3 is steep and negative for 2017 data however for 2003 the slope is very small but still positive. Comparing this to the IPM, mode L3's natural frequency, 0.746Hz, is within the bandwidth close to 0kg equivalent added mass for a lateral pacing frequency of 0.6Hz [19]. The polarity of this value is dependent on the walking frequency according to the IPM. Ref [37] suggests that an increase in crowd density decreases the pedestrian walking velocity. The 2003 event observed large crowd densities

on average on the walkways, 1.1people/m^2 at the estimated maximum number of people. This may have resulted in slow walking speeds potentially causing smaller pacing frequencies. However, the 2017 event observed low pedestrian densities on average on the roadway in comparison, 0.13people/m^2 at the estimated maximum number of people. This may have promoted faster walking speeds resulting in larger pacing frequencies (on average) suggesting equivalent negative added mass by pedestrians, according to the IPM [19]. This qualitatively agrees with the observed trend.

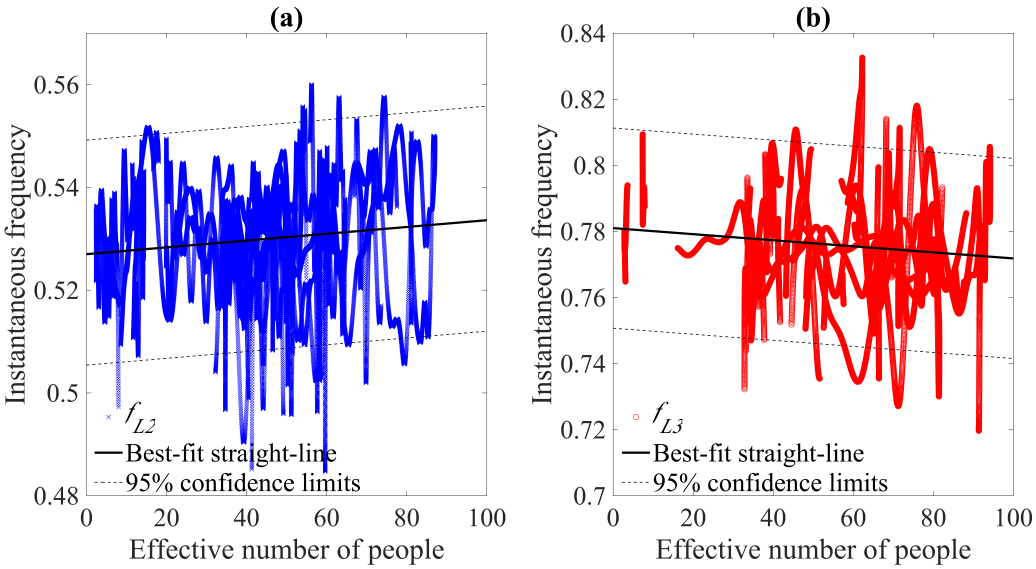

Figure 10: *2017 event - relationship between instantaneous frequency and effective number of pedestrians (a) Mode L2;(b) Mode L3*

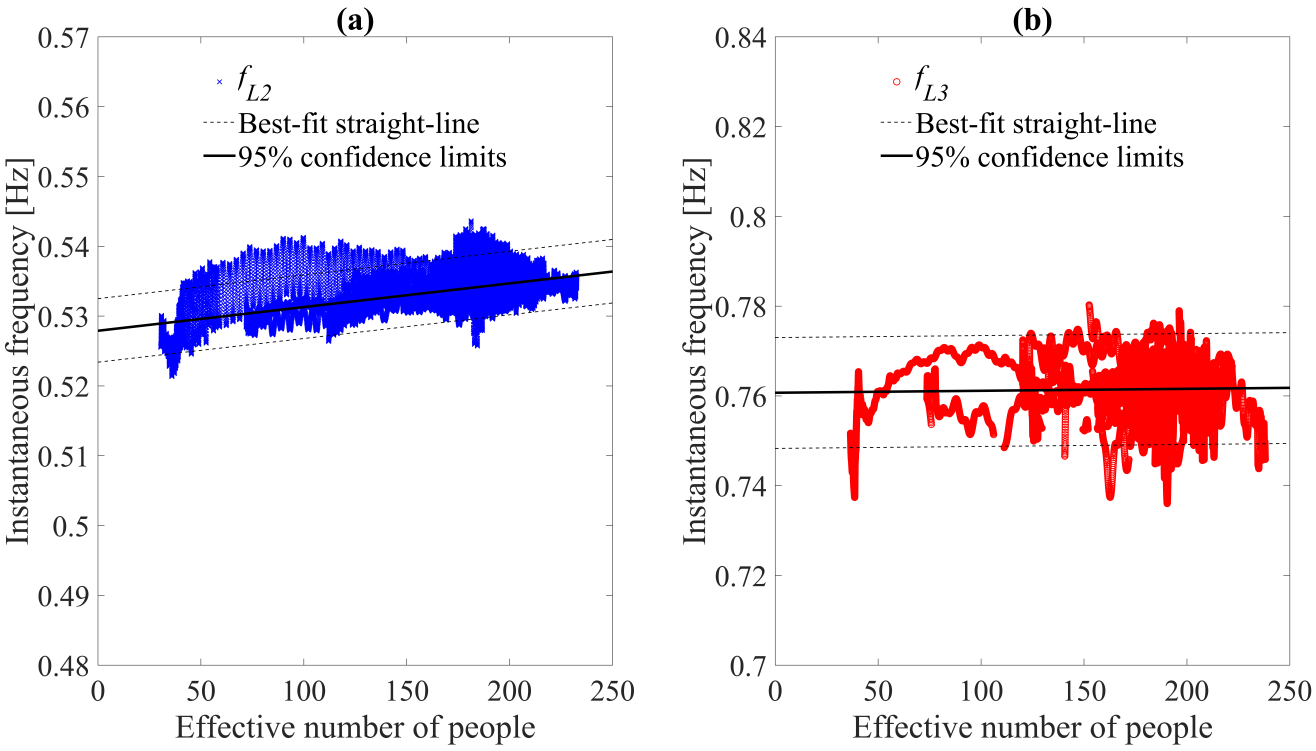

Figure 11: *2003 event - relationship between instantaneous frequency and effective number of pedestrians (a) Mode L2;(b) Mode L3*

Table 5: *Comparison of instantaneous frequency for 2003 and 2017 crowd loading events*

	L2			L3		
Dataset	correl. coeff. r	gradient, b [Hz/pedestrian] (10^{-5})	intercept, a [Hz]	correl. coeff. r	gradient, b [Hz/pedestrian] (10^{-5})	intercept, a [Hz]
2003	0.501	1.617	0.528	0.027	0.214	0.7607
2017	0.123	6.610	0.527	-0.13	-9.180	0.781

3.5 Arup's Negative Damping Model

This method of analysis considers the principle of conservation of energy assuming the energy input by pedestrians is output into the bridge directly corresponding to changes in the observed vibration amplitude from cycle-to-cycle. An equivalent force is assumed to account for the pedestrians' lateral forcing on the bridge deck. The equation used to identify the amplitude of the equivalent generalised lateral excitation force per pedestrian in phase with the bridge velocity, for each vibration cycle, is given by [1]:

$$F_{\mathrm{ped,v}}(t) = \frac{M_{q,b}}{N_{q.\mathrm{eff}}\sqrt{\psi}}\left(2\zeta_{q,b}A + \frac{\Delta A}{\pi}\right) \tag{16}$$

where A is the generalised acceleration vibration amplitude, ΔA is the increase in the amplitude from one cycle to the next.

The velocity amplitude used for this method of analysis was evaluated using the Hilbert Transform which is discussed in Section 3.2. Both the force and velocity amplitudes are scaled by $\sqrt{2}$ [1, 5] to be consistent with Arup's procedure of analysis. The full procedure can be found in reference[1]

The equation of motion of the bridge, for the q^{th} mode, is given by eqn (17). The forcing by the pedestrians, on the right-hand side of eqn (17), comprises three force component terms. A motion-independent static force, equivalent to that generated while walking on rigid ground, $F_{st}(t)$, and two motion-dependent force components of which one can be expressed as equivalent added mass, $F_{\mathrm{ped,a}}(t)$, and the other as equivalent added damping, $F_{\mathrm{ped,v}}(t)$. Arup's negative damping coefficient, k, corresponds to minus the average value of c_j per person ($\bar{c}_j \approx -k$). It is given by,

$$M_{q,b}\ddot{X}_q(t) + C_{q,b}\dot{X}_q(t) + K_{q,b}X_q(t) = F_{st}(t) - F_{\mathrm{ped,a}}(t) - F_{\mathrm{ped,v}}(t) \tag{17}$$

$$F_{\mathrm{ped,a}}(t) = \ddot{X}_q(t)\phi_q^2(x_j)\sum_{j=1}^{N_p}\alpha_{q,j}m_j(\omega_b), \quad F_{\mathrm{ped,v}}(t) = \dot{X}_q(t)\phi_q^2(x_j)\sum_{j=1}^{N_p}c_j(\omega_b) \tag{18}$$

where dots denote derivatives with respect to time, $C_{q,b}$ and is the bridge modal damping coefficient, $X_q(t)$ is the bridge modal displacement, $\alpha_{q,j}m_j$ is the equivalent added mass per pedestrian and ω_b is the circular vibration frequency of the bridge.

Arup's procedure (eqn (16)) is a method of approximating the third term on the right-hand side of the equation of motion (eqn (17)), $F_{\mathrm{ped,v}}(t)$, directly from measured bridge deck acceleration. This is an estimation which accepts that $F_{st}(t)$, cycle-to-cycle, contributes to the estimation of F_{ped}(t). The external forcing $F_{st}(t)$ is random in nature, due to the variability in step-by-step locomotion, which, on average, is zero. This can be described as a random walk [38]. For low-amplitude bridge vibrations, this makes it difficult to distinguish $F_{\mathrm{ped,v}}(t)$ from $F_{st}(t)$ for this method of analysis due to the significant scatter observed.

To evaluate the "lateral walking coefficient" (negative damping coefficient), $F_{\mathrm{ped,v}}$(t), (eqn (16) is plotted as a function of the locally scaled bridge deck velocity amplitude, as previously mentioned. The negative damping coefficient is directly evaluated from the gradient of this relationship. This gradient has been previously shown to be linear [1, 5, 6]. To reduce the effect of $F_{st}(t)$, in the identification of the negative damping coefficients of mode L2 and L3, F_{ped}(t) and $\dot{X}_{q,\mathrm{amp}}$(t) measurements were allocated into bins of 1x10^{-4} m/s^2 intervals and averaged, accordingly producing a single data point per bin.

The results from the procedure of Arup's negative damping model are illustrated in Figure 12. Figure 12(a) and Figure 12(b) display a linear trend for both modes L2 and L3 respectively, with 95% confidence limits. This qualitatively agrees with the literature [1, 4, 5, 6, 11, 12, 13, 14, 15]. The applicability of the negative damping model for low-amplitude bridge vibrations suggests that a threshold amplitude is not required for the HSI phenomenon observed during lateral bridge excitation. Outliers were still present using this method of analysis and were therefore omitted during the regression to obtain best approximates for the gradient '*k*' values, negative damping coefficients per pedestrian. These values were evaluated as -685Ns/m and -970Ns/m for modes L2 and L3 respectively. These are significantly larger than Macdonald's findings, from the 2003 experimental data [5], of -160Ns/m and -210Ns/m, for modes L2 and L3 respectively, and Arup's value of -300Ns/m from measurements on the LMF[1]. However, Macdonald suggested that at low amplitudes the gradient of mode L2 could possibly be significantly steeper [5]. From a series of measurements on a laterally oscillating treadmill, Ingólfsson et al. [11] considered the amplitude dependency of the added damping and mass coefficients, suggesting that they differ for low and high amplitude vibrations. Also, the level of noise observed (noise-signal ratio) in the measurements could cause inaccuracies which are amplified through the analysis, lading to uncertainty in the evaluation of the gradients in Figure 12.

Table 6 summarises the evaluated equivalent added mass and damping coefficients per pedestrian for both crowd loading events, 2003 and 2017 respectively.

Table 6: *Comparison of equivalent added mass and damping coefficients for 2003 and 2017 crowd loading events*

	2003		2017	
	k (Ns/m)	$\alpha_q \bar{m}_p$ (kg)	k (Ns/m)	$\alpha_q \bar{m}_p$ (kg)
L2	160	-71.5	685	-164
L3	210	6.70	970	174

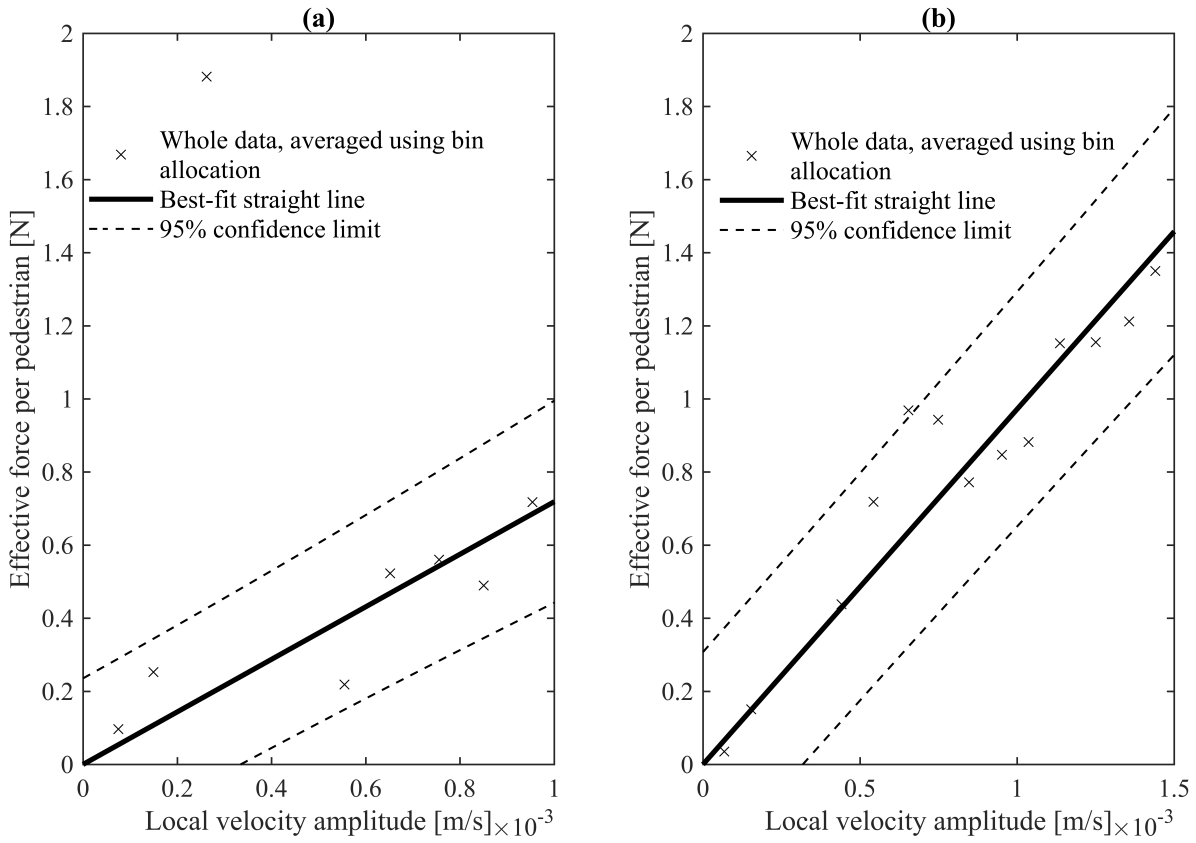

Figure 12: *Relationship between bridge velocity amplitude and force amplitude (in phase with velocity) per pedestrian: (a) Mode L2; (b) Mode L3*

4 Conclusions

A novel procedure has been presented to evaluate the equivalent added mass of pedestrians during crowd loading using a time-frequency analysis approach. This has enabled the mean equivalent added mass per person to be identified from full-scale data for the first time. Although some of the results are uncertain quantitatively, there is no evidence of a threshold amplitude at which the HSI phenomenon starts. Statistical analysis suggests tentative evidence for human-structure interactions observed at low amplitudes during the 2017 crowd loading event. Qualitatively this agrees well with the literature however, the quantification of the equivalent added mass and damping per pedestrian gives significantly large values. They have been difficult to identify accurately due to the noise-to-signal ratio and large scatter of the results at low amplitude.

A structure's total modal mass has been shown to decrease for an increase in the number of pedestrians for mode L2 in the 2003 crowd loading event. This is observed through an increase in the resonant

frequency of this mode for an increase in the number of people. The mean equivalent added mass per pedestrians has been approximated as 71.5kg for this mode.

Arup's negative damping model is inconclusive for the 2017 crowd loading event however equivalent negative added damping by pedestrians is observed. The applicability of this model for low-amplitude bridge responses is therefore uncertain. The estimation of the equivalent added damping includes the variation in amplitude from cycle-to-cycle, which at low amplitudes ignores information in the bridge response during each cycle. The bridge-independent forcing by pedestrians causes difficulty in extracting the negative damping coefficient observed during crowd loading.

5 Acknowledgements

The authors gratefully acknowledge: the Clifton Suspension Bridge Trust for the research opportunity and cooperation throughout installation and decommissioning of the Structural Health Monitoring System; the Bridgemaster Mrs Trish Johnson and the bridge maintenance staff for their assistance; Mr Sam Gunner for the installation and decommissioning of his bespoke Structural Health Monitoring System; Miss Xioyang Wang, Dr Ute Leonards and Mr Artur Soczawa-Stronczyk for assisting in the data collection; Dr Matt Dietz for consultation on data processing and spectral analysis and COWI for providing details of their Finite Element model. RW is supported by an EPSRC Doctoral Training Partnership studentship.

References

[1] P. Dallard, A. J. Fitzpatrick, A. Flint, S. Le Bourva, A. Low, R. Ridsdill Smith, and M. Willford, "The london millennium footbridge," *Structural Engineer*, vol. 79, no. 22, pp. 17–21, 2001.

[2] Y. Fujino, B. M. Pacheco, S.-I. Nakamura, and P. Warnitchai, "Synchronization of human walking observed during lateral vibration of a congested pedestrian bridge," *Earthquake Engineering & Structural Dynamics*, vol. 22, no. 9, pp. 741–758, 1993.

[3] F. Danbon and G. Grillaud, "Dynamic behaviour of a steel footbridge. characterization and modelling of the dynamic loading induced by a moving crowd on the solferino footbridge in paris," *Second International Conference on Footbridge (Proceedings), Venice, Italy,6-8 Decemeber*, 2005.

[4] E. Caetano, Á. Cunha, F. Magalhães, and C. Moutinho, "Studies for controlling human-induced vibration of the pedro e inês footbridge, portugal. part 1: Assessment of dynamic behaviour," *Engineering Structures*, vol. 32, no. 4, pp. 1069–1081, 2010.

[5] J. Macdonald, "Pedestrian-induced vibrations of the clifton suspension bridge, uk," *Proceedings of the Institution of Civil Engineers-Bridge Engineering*, vol. 161, no. 2, pp. 69–77, 2008.

[6] J. M. W. Brownjohn, P. Fok, M. Roche, and P. Omenzetter, "Long span steel pedestrian bridge at singapore changi airport. part 2: Crowd loading tests and vibration mitigation measures," *The Structural Engineer*, vol. 82, no. 16, pp. 28–34, 2004.

[7] A. D. Pizzimenti and F. Ricciardelli, "Experimental evaluation of the dynamic lateral loading of footbridges by walking pedestrians," *Sixth International Conference on Structural Dynamics, Paris, France, 4-7 September*, 2005.

[8] R. H. Scanlan and J. Tomo, "Air foil and bridge deck flutter derivatives," *Journal of Soil Mechanics & Foundations Div*, vol. 97, no. 6, pp. 1717–1737, 1971.

[9] N. Nikitas, J. H. G. Macdonald, and J. B. Jakobsen, "Identification of flutter derivatives from full-scale ambient vibration measurements of the clifton suspension bridge," *Wind and Structures*, vol. 14, no. 3, pp. 221–238, 2011.

[10] J. H. G. Macdonald, "Lateral excitation of bridges by balancing pedestrians," *Proceedings of the Royal Society A: Mathematical, Physical and Engineering Sciences*, vol. 465, no. 2104, pp. 1055–1073, 2008.

[11] E. T. Ingólfsson, C. T. Georgakis, F. Ricciardelli, and J. Jönsson, "Experimental identification of pedestrian-induced lateral forces on footbridges," *Journal of Sound and Vibration*, vol. 330, no. 6, pp. 1265–1284, 2011.

[12] M. Bocian, J. H. G. Macdonald, J. F. Burn, and D. Redmill, "Experimental identification of the behaviour of and lateral forces from freely-walking pedestrians on laterally oscillating structures in a virtual reality environment," *Engineering structures*, vol. 105, pp. 62–76, 2015.

[13] M. Bocian, J. F. Burn, J. H. G. Macdonald, and J. M. W. Brownjohn, "From phase drift to synchronisation–pedestrian stepping behaviour on laterally oscillating structures and consequences for dynamic stability," *Journal of Sound and Vibration*, vol. 392, pp. 382–399, 2017.

[14] S. P. Carroll, J. S. Owen, and M. F. Hussein, "Reproduction of lateral ground reaction forces from visual marker data and analysis of balance response while walking on a laterally oscillating deck," *Engineering Structures*, vol. 49, pp. 1034–1047, 2013.

[15] S. P. Carroll, J. S. Owen, and H. M. F, "Experimental identification of the lateral human–structure interaction mechanism and assessment of the inverted-pendulum biomechanical model," *Journal of Sound and Vibration*, vol. 333, no. 22, pp. 5865–5884, 2014.

[16] C. Barker, "Some observations on the nature of the mechanism that drives the self-excited lateral response of footbridges," *First International Conference of (Proceedings) Footbridge, Paris, France, 20–22*, 2002.

[17] D. A. Winter, "Human balance and posture control during standing and walking," *Gait & posture*, vol. 3, no. 4, pp. 193–214, 1995.

[18] C. E. Bauby and A. D. Kuo, "Active control of lateral balance in human walking," *Journal of biomechanics*, vol. 33, no. 11, pp. 1433–1440, 2000.

[19] M. Bocian, J. H. G. Macdonald, and J. Burn, "Biomechanically inspired modelling of pedestrian-induced forces on laterally oscillating structures," *Journal of Sound and Vibration*, vol. 331, no. 16, pp. 3914–3929, 2012.

[20] W. H. Barlow, "Description of the clifton suspension bridge (including plate)," *Minutes of the Proceedings of the Institution of Civil Engineers*, vol. 26, no. 26, pp. 243–257, 1867.

[21] S. Gunner, P. J. Vardanega, T. Tryfonas, J. H. G. Macdonald, and R. E. Wilson, "Rapid deployment of a WSN on the clifton suspension bridge, uk," *Proceedings of the Institution of Civil Engineers-Smart Infrastructure and Construction*, vol. 170, no. 3, pp. 59–71, 2017.

[22] R. Hollamby, "Clifton suspension bridge finite element model," 2010. COWI, Gloucestershire, UK.

[23] m_c8bit, "Timestamp," 29 March 2017. `https://play.google.com/store/apps/details?id=jp.m_c8bit.timestamp&hl=en_US` (Accessed October 2017).

[24] B. J. Mohler, W. B. Thompson, S. H. Creem-Regehr, H. L. Pick Jr, and W. H. Warren Jr, "Visual flow influences gait transition speed and preferred walking speed," *Experimental brain research*, vol. 181, no. 2, pp. 221–228, 2007.

[25] R. C. Browning, E. A. Baker, J. A. Herron, and R. Kram, "Effects of obesity and sex on the energetic cost and preferred speed of walking," *Journal of applied physiology*, vol. 100, no. 2, pp. 390–398, 2006.

[26] A. E. Minetti, "The three modes of terrestrial locomotion," *Biomechanics and biology of movement*, pp. 67–78, 2000.

[27] T. Ji and A. Pachi, "Frequency and velocity of people walking," *Structural Engineer*, vol. 84, no. 3, pp. 36–40, 2005.

[28] N. H. S, "National health service, health survey for england 2008 trend tables." `/http://www.ic.nhs.uk/pubs/hse08trendsS/`, 2009. (accessed November 2017).

[29] MatLab, "Signal processing toolbox," 2017. The MathWorks Inc., Natick, MA, USA.

[30] L. Marple, "Computing the discrete-time "analytic" signal via fft," *IEEE Transactions on signal processing*, vol. 47, no. 9, pp. 2600–2603, 1999.

[31] J. G. Proakis, *Digital signal processing: principles algorithms and applications*. Pearson Education India, 2001.

[32] P. Welch, "The use of fast fourier transform for the estimation of power spectra: a method based on time averaging over short, modified periodograms," *IEEE Transactions on audio and electroacoustics*, vol. 15, no. 2, pp. 70–73, 1967.

[33] M. T. Taner, F. Koehler, and R. E. Sheriff, "Complex seismic trace analysis," *Geophysics*, vol. 44, no. 6, pp. 1041–1063, 1979.

[34] F. J. Harris, "On the use of windows for harmonic analysis with the discrete fourier transform," *Proceedings of the IEEE*, vol. 66, no. 1, pp. 51–83, 1978.

[35] M. G. Kendall and A. Stuart, *The Advanced Theory of Statistics. Vols. II and III.* Edward Arnold Publishers Ltd, 1961.

[36] S. Bhattacharya, N. A. Alexander, D. Lombardi, and S. Ghosh, *Fundamentals of Engineering Mathematics*. ICE, 2017.

[37] Z. Fang, S. M. Lo, and J. A. Lu, "On the relationship between crowd density and movement velocity," *Fire Safety Journal*, vol. 38, no. 3, pp. 271–283, 2003.

[38] K. Pearson, “The problem of the random walk,” *Nature*, vol. 72, no. 1867, p. 342, 1905.